

## Monte Carlo simulation of interface alloying

Carlos Frontera, Eduard Vives, Teresa Castán, and Antoni Planes

*Departament d'Estructura i Constituents de la Matèria, Facultat de Física, Universitat de Barcelona, Diagonal 647, 08028 Barcelona, Catalonia, Spain*

(Received 23 September 1994)

An Ising-like model, with interactions ranging up to next-nearest-neighbor pairs, is used to simulate the process of interface alloying. Interactions are chosen to stabilize an intermediate "antiferromagnetic" ordered structure. The dynamics proceeds exclusively by atom-vacancy exchanges. In order to characterize the process, the time evolution of the width of the intermediate ordered region and the diffusion length is studied. Both lengths are found to follow a power-law evolution with exponents depending on the characteristic features of the model.

### I. INTRODUCTION

Interface alloying of two metals is a nonequilibrium problem of great interest because of its relation with technological processes like diffusion bonding, thin film deposition, and laser surface alloying. Generically, interface alloying appears when two soluble metals with similar crystallographic structures and lattice parameters are put in close contact. Atomic interdiffusion of the two species  $A$  and  $B$  may appear, and eventually, a new intermediate phase mixture of  $A$  and  $B$  arises. The structure of this intermediate phase can be very complex and depends, among other parameters, on the microscopic interactions between  $A$  and  $B$  atoms. The effect of these interactions is measured in terms of the effective mixing energy  $J$ . For low temperatures, the case  $J < 0$  prevents the interdiffusion and so no intermediate structure is formed. When the interactions between both species are negligible ( $J = 0$ ) or the temperature is very high, the new phase is a random solution of  $A$  and  $B$  atoms. In this paper we focus on the more interesting case of  $J > 0$ . Then, for temperatures low enough, the arising intermediate phase is an ordered structure with a certain periodicity like the so-called  $B2$  or  $DO_3$  structures observed in bcc crystals.

Experimental examples can be found when a thin film is deposited on a substrate, like Sn-Pt which forms an intermediate  $DO_3$  structure,<sup>1</sup> Al-Ni which may form a rich variety of ordered structures,<sup>2</sup> and Co-Pt which forms a random solution.<sup>3</sup> Other examples are laser surface alloying like the case of Fe-Cr,<sup>4</sup> and superlattice structure growth.<sup>5</sup> It is also worth mentioning the case of the two semiconductors AuGe and GaAs which form an Au-Ga alloy.<sup>6</sup> A related problem is the Kirkendall effect,<sup>7</sup> which appears when the two species  $A$  and  $B$  diffuse at different rates.

Besides its metallurgic relevance, this problem is also very interesting from a more fundamental point of view. Indeed, interface alloying of two metals can be regarded as the relaxation from an initially ordered but unstable phase (two pure  $A$  and  $B$  phases separated by a flat inter-

face), to a final equilibrium phase exhibiting a different order. This case represents a step forward from the standard experiments, in which the system is in an initially disordered state, which have been extensively studied by different methods.<sup>8</sup> They are schematically indicated in Fig. 1(a) by the arrows I (order-disorder) and II (phase separation). In our case (represented by arrow III) the understanding of the intermediate path, joining both the initially unstable and the final stable ordered structures, may provide a new insight into the dynamics of nonequilibrium ordering phenomena.

In this paper, a simple microscopic model is formulated in terms of Ising-like variables, and it is used to study the formation and growth of the intermediate ordered phase arising when two pure  $A$  and  $B$  phases are put in close contact. We have restricted ourselves to a two dimensional (2D) case and considered pair interactions only, ranging up to next-nearest neighbors. The dynamical evolution is studied by Monte Carlo simulation and we have incorporated the important fact that in binary alloys the diffusion proceeds via vacancies.<sup>9</sup> Although, in most of the cases, the concentration of vacancies is very small and it is not expected to modify substantially the equilibrium properties of the system, they turn out to be crucial in the dynamics. Indeed, in recent simulations of the order-disorder process, the vacancy mechanism has been shown to increase the domain growth exponent compared to the standard atom-atom exchange mechanism, provided that the range of microscopic dynamics extends, at least, up to next-nearest neighbors.<sup>10</sup> It should be mentioned that a similar model has been previously proposed for the study of interface alloying using Monte Carlo simulations but incorporating a different algorithm for the vacancy dynamics.<sup>11,12</sup> As a consequence of this difference, it is not straightforward to compare their results with ours, which seem, in some cases, contradictory. This will be discussed in Secs. II and IV.

Given the complexity of the phenomenon when considering real materials, one should not expect to compare directly simulations with experiments. Nevertheless, the model allows the possibility of studying the ef-

fect of both the microscopic chemical interactions and the dynamic rules on the relaxation path. It should also be mentioned that to our knowledge no experimental attempts at characterizing quantitatively the dynamics of such process have been performed. There are, nevertheless, some experiments where the process is qualitatively described.<sup>1-4,6</sup>

From our results, the relaxation process can be characterized by the time evolution of three relevant lengths indicated in Fig. 1(b): the size of the intermediate ordered structure  $\delta$ , the diffusion length  $\lambda$  of the  $A(B)$  atoms in

the  $B(A)$  phase, and finally the roughness of the interface  $W$  between the two ordered (stable and unstable) phases. Here we shall focus on the ordering process itself rather than on the characteristics of the interface. The analysis of the parameter  $W$  together with the eventual fractal properties of the interface will be presented elsewhere.

The paper is organized in the following manner: first, in Sec. II, we introduce the model and provide information about the simulation procedure. In Sec. III we present the obtained results and finally in Sec. IV we discuss and give the conclusions.

## II. MODEL AND MONTE CARLO SIMULATION DETAILS

The atomic configuration of the alloy is described by a set of spin variables  $\{S_{ij}\}$  ( $i = 1, 2, \dots, L_x, j = 1, 2, \dots, L_y$ ) on a 2D square lattice. Each spin can take three values:  $S_{ij} = 1$  for an  $A$  atom,  $S_{ij} = -1$  for a  $B$  atom, and  $S_{ij} = 0$  for a vacancy. The following Hamiltonian is proposed:

$$H = J_1 \sum_{\text{n.n.}} S_{ij} S_{kl} - J_2 \sum_{\text{n.n.n.}} S_{ij} S_{kl}, \quad (1)$$

where the first sum extends over all nearest-neighbor (n.n.) pairs and the second sum over all the next-nearest-neighbor (n.n.n.) pairs.  $J_1$  and  $J_2$  are taken to be non-negative constants in order to ensure the antiferromagnetic ( $ABABA$ ) order of the low-temperature equilibrium state. By taking  $J_1$  as the unit of energy we can write the reduced Hamiltonian as

$$H/J_1 \equiv H^* = \sum_{\text{n.n.}} S_{ij} S_{kl} - K^* \sum_{\text{n.n.n.}} S_{ij} S_{kl}. \quad (2)$$

Three different values of the ratio  $K^* = J_2/J_1$  have been considered:  $K^* = 0, 0.5,$  and  $1.0$ . For such a simplified model, this parameter  $K^*$  can be understood as an effective interaction range. Simulations have been performed on a  $L_x = 100 \times L_y = 300$  lattice ( $N = L_x \times L_y$ ) with  $N_A = 14999$  (number of  $A$  atoms),  $N_B = 15000$  (number of  $B$  atoms), and  $N_V = 1$  (number of vacancies). This represents a very low concentration of vacancies ( $\sim 3.3 \times 10^{-5}$ ) as is expected for a metallic system. Actually, the effect of introducing more vacancies has been studied in the case of a quench of type I [see Fig. 1(a)] and does not influence significantly the dynamics.<sup>13</sup> The initial state consists of two pure  $A$  and  $B$  phases separated by a flat interface initially located at the position  $j = 150$ .

The dynamics is performed by exchanging atoms with the vacancy only. Hereafter we shall refer to this exchanges as “vacancy jumps.” Such jumps can be performed either to n.n. or to n.n.n. positions. The ratio of n.n.n. proposed vacancy jumps relative to the total number of proposed jumps is defined as

$$Q \equiv \frac{\text{number of proposed jumps to n.n.n.}}{\text{total number of proposed jumps}}. \quad (3)$$

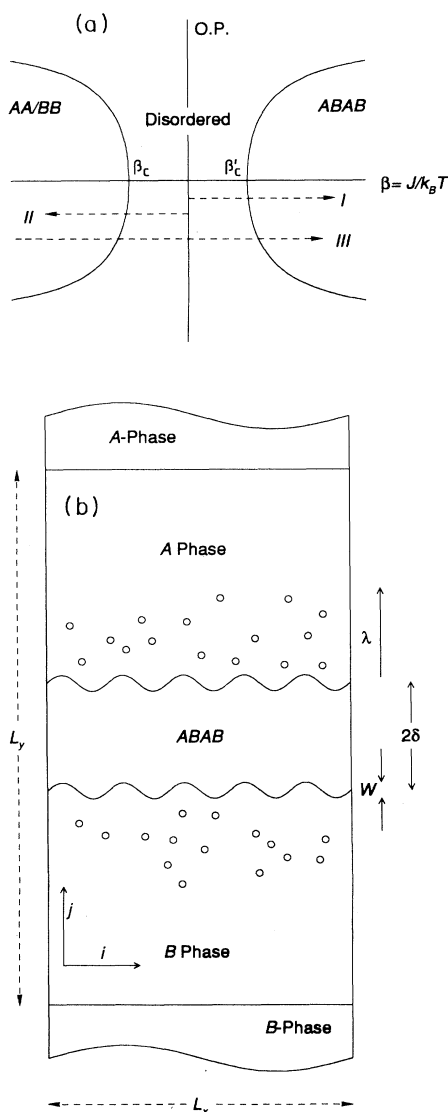


FIG. 1. (a) Schematic phase diagram for an Ising binary alloy representing the different quench experiments discussed in the text. The vertical axis represents the generic order parameter.  $\beta_c$  and  $\beta'_c$  are the ferromagnetic and antiferromagnetic critical points, respectively. (b) Schematic representation of the simulated system indicating the relevant lengths  $W$ ,  $\lambda$ , and  $\delta$ . Open circles represent diffused  $A(B)$  particles inside the  $B(A)$  phase.

Two values of  $Q$  have been considered:  $Q = 0$  (vacancy jumps to n.n.n. positions are not allowed) and  $Q = 0.5$  (vacancy jumps to n.n. and to n.n.n. positions proposed with the same probability). In real systems this ratio is controlled by the values of the barrier heights associated to each path. Thus, the parameter  $Q$  is an effective measure of the range of the average vacancy jump, which in general will depend on both the temperature and the special features of each system.

The vacancy jumps are accepted following the standard Metropolis probability:

$$P = \text{Min}\{1, \exp(-\Delta H/k_B T)\}, \quad (4)$$

with  $k_B T/J_1 = 1.0$ . This temperature is low enough compared to the critical temperature of the order-disorder transition ( $T/T_c < 0.5$ ) for all the studied values of  $J_2$ , in order to ensure that critical fluctuations are irrelevant.

Notice that with this probability (4) the vacancy is allowed to remain in the same position after the jump trial. This algorithm differs from the one used in Refs. 11, 12. In these works, the authors use a probability which always forces the vacancy to jump to one of its neighbours. This makes the acceptance ratio of the proposed jumps homogeneous and independent of the local state of order of the system which, *a priori*, cannot be assumed.

We have considered periodic boundary conditions along the  $i$  direction. Along the  $j$  direction fixed boundary conditions are imposed maintaining pure  $A$  and  $B$  phases. Concerning the vacancy, it is reflected every time it reaches the fixed boundaries. We define the unit of time (Monte Carlo step) as  $N$  vacancy jump trials. In order to study the evolution of the system we have measured the following quantities as a function of time:

(a) *Concentration profile*. It is measured averaging the concentration over  $i$  on rows of constant  $j$ :

$$c(j) \equiv \frac{1}{L_x} \sum_{i=1}^{L_x} S_{ij}. \quad (5)$$

(b) *Order parameter profile*. It is the absolute value of the antiferromagnetic order parameter measured on the rows with constant  $j$ :

$$m(j) \equiv \frac{1}{L_x} \left| \sum_{i=1}^{L_x} (-1)^i S_{ij} \right|. \quad (6)$$

(c) *Structure factor*.

$$S(k_x, k_y) = \left| \frac{1}{N} \sum_{l,m} S_{lm} e^{2\pi i(lk_x + mk_y)} \right|^2, \quad (7)$$

where  $1 \leq m \leq L_x$  and  $1 \leq l \leq L_y$  scan the direct lattice and  $0 \leq k_x < 1$  and  $0 \leq k_y < 1$  scan the reciprocal lattice. We have focused on the antiferromagnetic peak around the position  $\mathbf{k} = (1/2, 1/2)$  along the  $(0,1)$  direction.

### III. RESULTS

Figure 2 displays a comparative study of the evolution of the system for different values of the effective interaction range  $K^*$  and the microscopic dynamic range  $Q$ . Black symbols represent particles with a local environment neither in pure  $A$ , pure  $B$ , nor  $ABAB$  phase. It can be observed that when  $Q = 0$  the growth of the intermediate  $ABAB$  ordered phase is almost prevented while when  $Q = 0.5$  the width of the intermediate ordered region ( $\delta$ ) grows independently of the value of  $K^*$ . This is because n.n.n. vacancy jumps are needed to allow the vacancy to travel across the  $ABAB$  region in order to transport particles from the pure phases to the interface.<sup>10</sup> It can also be seen that  $K^*$  controls the diffusion of the  $A$  ( $B$ ) particles in the  $B$  ( $A$ ) phase. Actually, the diffusion length ( $\lambda$ ) decreases with increasing  $K^*$ . The reason for this behaviour has to do with the energy associated with an impurity inside the pure phase which increases linearly with  $K^*$ . The existence of antiphase boundaries inside the intermediate ordered phase which eventually will disappear at long times should be noticed [see Fig. 2(e)].

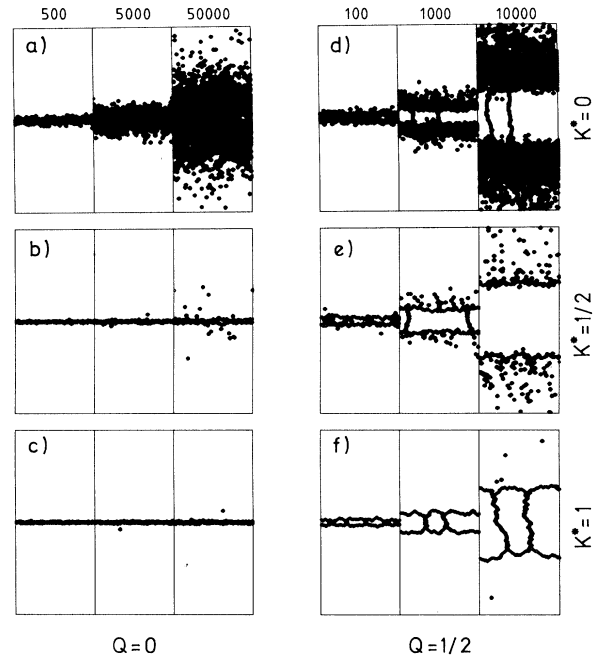


FIG. 2. Snapshots showing the evolution of the interface between two mutually soluble metals obtained by a Monte Carlo simulation. Black symbols represents particles neither in pure  $A$ , pure  $B$ , nor  $ABAB$  phase. The numbers on top indicate the time in Monte Carlo steps. The six different evolutions, from (a) to (f), correspond to  $k_B T/J_1 = 1.0$  and the following values of  $Q$  and  $K^*$ : (a)  $Q = 0$ ,  $K^* = 0$ ; (b)  $Q = 0$ ,  $K^* = 1/2$ ; (c)  $Q = 0$ ,  $K^* = 1$ ; (d)  $Q = 1/2$ ,  $K^* = 0$ ; (e)  $Q = 1/2$ ,  $K^* = 1/2$ ; (f)  $Q = 1/2$ ,  $K^* = 1$ . To refer to the six studied cases this terminology is kept in the next figures. The values of  $K^*$  and  $Q$  are indicated on the right and the bottom margins, respectively.

### A. Concentration, order parameter, and structure factor

A quantitative analysis of the behavior displayed in Fig. 2 can be carried out by studying the evolution of the concentration [Eq. (5)] and of the order parameter [Eq. (6)] profiles which are shown in Figs. 3 and 4, respectively. The curves have been averaged over ten independent runs and correspond to the same temporal sequences shown in Fig. 2. Moreover, the mirror symmetry existing at  $j = 150$  allows us to average the two equivalent regions and to display only half of the system. In the following, we redefine  $j$  starting at 1 in the middle of the system and ending at 150. In Figure 3, the width of the intermediate ordered region  $\delta$  can be estimated from the length of the plateau with  $c(j) \sim 0$ , while the diffusion length  $\lambda$  from the exponential increase towards  $c(j) \sim 1$ . These two relevant lengths have been obtained by fitting the following expression:

$$c(j) = \begin{cases} 0 & \text{when } j \leq \delta, \\ 1 - \exp\left(-\frac{j-\delta}{\lambda}\right) & \text{when } j \geq \delta. \end{cases} \quad (8)$$

The same lengths can also be obtained from the order parameter profiles plotted in Fig. 4. In this case,  $\delta$  can be estimated by measuring the width at half height and  $\lambda$  is related with the tail towards  $m(j) \simeq 0$ . It should be mentioned that the existence of antiphase domains prevents the order parameter from reaching its maximum

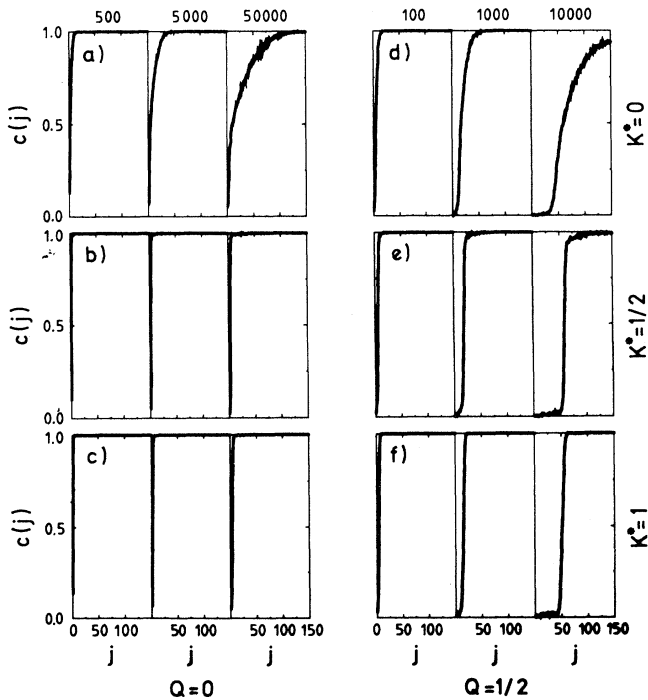


FIG. 3. Time evolution of the concentration profile for the six studied cases. The data correspond to an average over ten independent evolutions and furthermore each one of them is an average over the two antisymmetric half parts of the system.

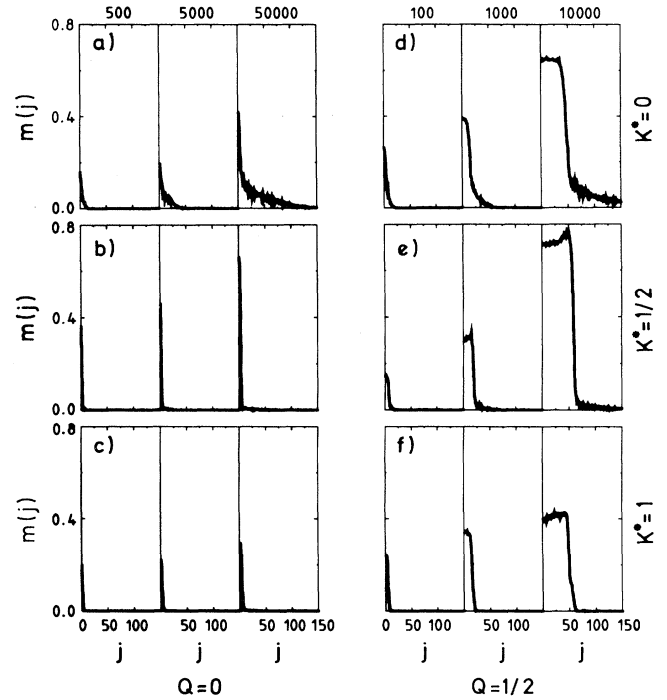


FIG. 4. Time evolution of the antiferromagnetic order parameter profile for the six studied cases. The averages have been performed over ten independent evolutions and furthermore each one of them is an average over the two symmetrical half parts of the system.

value  $m = 1$  in the intermediate ordered region. The overshooting that can be observed in some order parameter profiles [see, for instance Figs. 4(e) and 4(f)] might be related to the rough character of the interface and especially to the penetration of the pure phase in the antiphase domain boundaries that can be well appreciated in Fig. 2(f).

Figure 5 shows a linear-logarithmic plot of the structure factor along the  $(0,1)$  direction around the  $\mathbf{k} = (1/2, 1/2)$  position for the same time sequences as in the previous figures. They correspond to averages over 20 different independent runs. The emerging peak and the general oscillating character are a consequence of the growth of the intermediate ordered region. The width of

TABLE I. Exponents  $n$  characterizing the growth of  $\delta$ . The symbols correspond to those in Fig. 6.

	$Q = 0$	$Q = 1/2$
$K^* = 0$	○ 0.13	○ 0.49
	■ 0.12	■ 0.58
	△ 0.32	△ 0.55
$K^* = 1/2$	○ 0.06	○ 0.46
	■ 0.03	■ 0.54
	△ 0.12	△ 0.53
$K^* = 1$	○ 0.12	○ 0.48
	■ 0.13	■ 0.55
	△ 0.13	△ 0.53

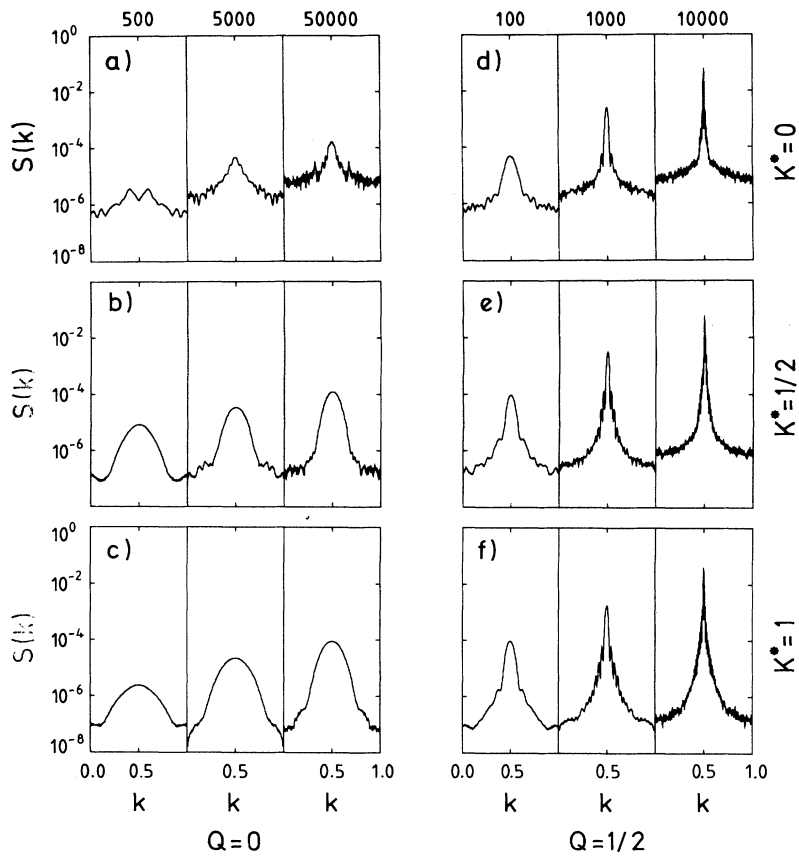


FIG. 5. Time evolution of the structure factor  $S(k)$  for the six studied cases. Data correspond to the line  $k = (1/2, k)$  and are shown in linear-logarithmic scale. The displayed results have been averaged over 20 independent runs.

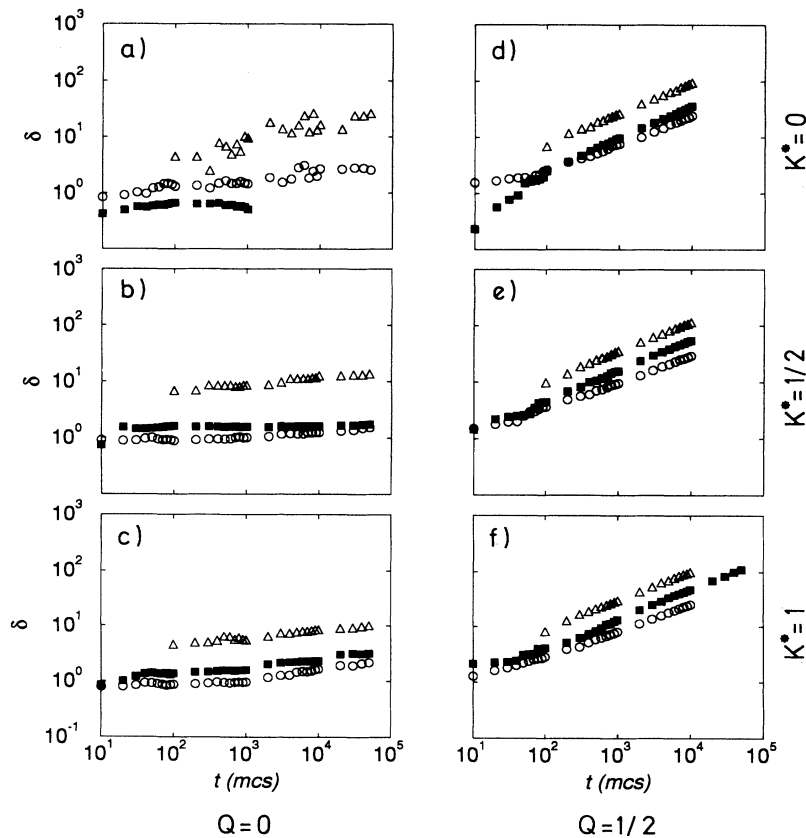


FIG. 6. Log-log plot of the time evolution of the width of the intermediate ordered region  $\delta$  for the six studied cases (mcs stands for Monte Carlo steps). Different symbols correspond to estimations from the concentration profiles (■), the order parameter profiles (○), and the structure factor (△).

the peak is proportional to the inverse of  $\delta$ . The main effect of the diffusion inside the pure phases is to enhance the background  $S_b$  as can be clearly seen in Figs. 5(a) and 5(d). It can be assumed that  $S_b \sim L_x \lambda$ .

### B. Time evolution of $\delta$ and $\lambda$

Figure 6 shows, in a log-log plot, the time evolution of the width of the intermediate region ( $\delta$ ) for the different values of the model parameters  $Q$  and  $K^*$ . Different symbols correspond to estimations obtained from the concentration (■), the order parameter (○), and the structure factor ( $\Delta$ ). After a short transient,  $\delta$  increases with time following a power law characterized by an exponent  $n$  ( $\delta \sim t^n$ ). Table I summarizes the values of  $n$  for all the displayed cases. The different estimations agree in all the cases except for case (a) where the estimation from the structure factor gives a larger value of  $n$ . This is due to the strong effect of the diffusion background which masks the tiny growth of the width of the peak  $\delta^{-1}$ . Despite this, the results obtained are compatible with a value of  $n = 0.52 \pm 0.05$  for  $Q = 1/2$  and  $n = 0.13 \pm 0.08$  for  $Q = 0$  irrespective of the value of  $K^*$ . This fact is in complete agreement with the qualitative explanation advanced at the beginning of this section; that is,  $Q = 0$  prevents the vacancy movements across the ordered region, and so the growth is strongly slowed down.

Figure 7 shows the time evolution of the diffusion length  $\lambda$  for the different values of  $Q$  and  $K^*$  obtained

TABLE II. Exponents  $p$  characterizing the growth of  $\lambda$ . The symbols correspond to those in Fig. 7.

	$Q = 0$	$Q = 1/2$
$K^* = 0$	■ 0.45 $\Delta$ 0.52	■ 0.46 $\Delta$ 0.50
$K^* = 1/2$	■ 0.24 $\Delta$ 0.08	■ 0.22 $\Delta$ 0.19
$K^* = 1$	■ 0.19 $\Delta$ 0.01	■ 0.27 $\Delta$ 0.30

from the concentration profile (■) and from the structure factor background ( $\Delta$ ). It has not been possible to obtain reliable estimations of this quantity from the order parameter since the diffusion tail in  $m(j)$  is too small. The results are compatible with a power-law growth for  $\lambda$  characterized by an exponent  $p$  ( $\lambda \sim t^p$ ). The numerical results, shown in Table II, are consistent with a value  $p = 0.50 \pm 0.05$  for  $K^* = 0$  and  $p = 0.23 \pm 0.07$  for  $K^* \neq 0$  independently of  $Q$ . Again this is in agreement with the qualitative description given at the beginning of this section, suggesting that the diffusion is drastically reduced (by a factor around 2 in the exponent  $p$ ) when the interactions to n.n.n.'s are switched on ( $K^* \neq 0$ ). The values of  $p$  obtained from the structure factor in cases (b) and (c) are doubtful since the low diffusion makes difficult to discriminate the background from the very wide peak (see Fig. 5).

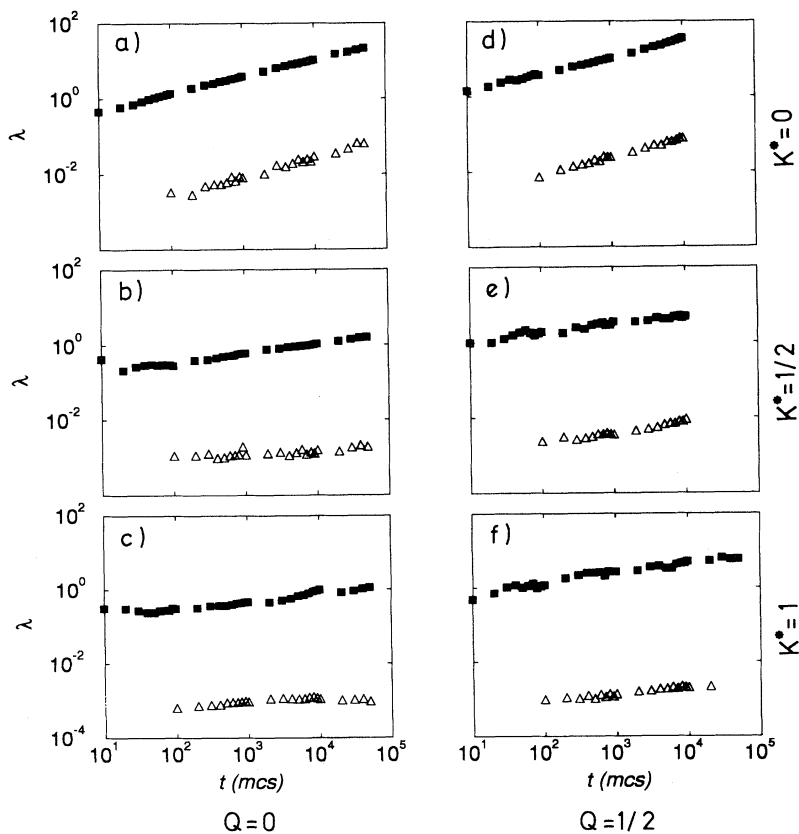


FIG. 7. Log-log plot for the time evolution of the diffusion length  $\lambda$  for the six studied cases. Different symbols correspond to estimations from the concentration profiles (■) and the structure factor ( $\Delta$ ).

#### IV. DISCUSSION AND CONCLUSIONS

From the results of Table I, one can conclude that the exponent for the growth of the width of the intermediate phase is  $n = 1/2$  provided that the vacancy is allowed to jump to n.n.n.'s ( $Q \neq 0$ ). This result can be theoretically explained assuming that during the evolution, the relaxation of the order parameter is much faster than the relaxation of the concentration. This assumption is justified taking into account that ordering does not require long-range diffusion so that the coarse-grained value of the local order parameter can rapidly reach, at every time, its maximum value  $m \simeq \pm(1 - |c|)$ . As the relaxation of  $c$  is known to obey a diffusion equation, this leads to a growth  $\delta \sim t^{1/2}$ .<sup>14</sup>

It has already been mentioned that when  $Q = 0$  almost no proposed vacancy jumps are accepted inside the ordered region and so the growth of  $\delta$  is hindered. The picture we have in mind is that when the vacancy in the interface (pure-phase-*ABAB*-phase) cannot penetrate inside the ordered region (and consequently cannot cross the intermediate ordered region) it travels along the interface or towards the pure phase. During this process, the vacancy transports particles from the interface to the pure phase, destroying the *ABAB* phase partially, so that almost no net increasing of  $\delta$  can be observed.

From Table II one can conclude that the growth of the diffusion length  $\lambda$  obeys a power law with  $p = 1/2$  when  $K^* = 0$ , as expected from a pure diffusion of the  $A(B)$  particles inside the  $B(A)$  phase. When  $K^* \neq 0$  the diffusion is prevented mainly because of the tendency for the diffusing particles to aggregate in n.n.n. positions (with an energy gain of  $K^*$ ). This fact can be naively

compared to the existence of a random potential that it is known to decrease the diffusion exponent.<sup>15</sup> Such a decrease in the diffusion when  $K^* \neq 0$  was already pointed out in Ref. 12.

In summary, a kinetic model for the study of interface alloying via vacancies has been proposed. It allows one to simultaneously study the effect of both the interaction and the dynamic ranges on the growth of the intermediate ordered region as well as the diffusion length inside the initial pure phases. It has been shown that the growth of the intermediate ordered region follows a power law with an exponent  $1/2$  if the mobility of the vacancy prevents it from being trapped in the ordered regions. The diffusion of  $A(B)$  particles inside the  $B(A)$  phases is controlled by the mixing energy between the two species. When the range of the interaction is long enough, diffusion is prevented. Otherwise the diffusion length grows following a power law, with an exponent  $1/2$ .

#### ACKNOWLEDGMENTS

We acknowledge J.M. Sancho for fruitful comments, the Fundació Catalana per a la Recerca (FCR), and the Centre de Supercomputació de Catalunya (CESCA) for computing facilities, and the Comisión Interministerial de Ciencia y Tecnología (CICYT) for financial support (Project No. MAT92-884). C.F. also acknowledges financial support from the Comissionat per a Universitats i Recerca (Generalitat de Catalunya).

<sup>1</sup> M. Galeotti, A. Atrei, U. Bardi, G. Rovida, and M. Torrini, *Surf. Sci.* **313**, 349 (1994).

<sup>2</sup> S.H. Lu, D. Tian, Z.Q. Wang, Y.S. Li, and F. Jona, *Solid State Commun.* **67**, 325 (1988).

<sup>3</sup> M. Galeotti, A. Atrei, U. Bardi, B. Cortiagiani, G. Rovida, and M. Torrini, *Surf. Sci.* **297**, 202 (1993).

<sup>4</sup> J. Liu, *Mater. Lett.* **15**, 53 (1992).

<sup>5</sup> N. Ikarashi, K. Akimoto, and T. Tatsumi, *Phys. Rev. Lett.* **72**, 3198 (1994).

<sup>6</sup> C.S. Fang, Y.L. Chang, and W.S. Tse, *Appl. Phys. A* **49**, 285 (1989).

<sup>7</sup> P. Haasen, *Physical Metallurgy* (Cambridge University Press, Cambridge, England, 1978).

<sup>8</sup> J.D. Gunton, M. San Miguel, and P.S. Sahni, in *Phase Transitions and Critical Phenomena*, edited by C. Domb and J.L. Lebowitz (Academic, London, 1983), Vol. 8.

<sup>9</sup> T. Eguchi, Y. Tomokiyo, and C. Kinoshita, *J. Phys. (Paris) Colloq. C7* **38**, 328 (1977), and references therein.

<sup>10</sup> E. Vives and A. Planes, *Phys. Rev. Lett.* **68**, 812 (1992); *Int. J. Mod. Phys. C* **4**, 701 (1993).

<sup>11</sup> V.B. Shapozhnikov and M.G. Goldiner, *J. Phys. A* **24**, L853 (1991).

<sup>12</sup> V.B. Shapozhnikov, *J. Phys. A* **26**, L1011 (1993).

<sup>13</sup> C. Frontera, E. Vives, and A. Planes, *Phys. Rev. B* **48**, 9321 (1993). For a studied range of the vacancy concentration ( $10^{-4}$ – $10^{-6}$ ) we do not find any significant change in the dynamical exponent.

<sup>14</sup> A. Onuki, K. Sekimoto, and D. Jasnow, *Prog. Theor. Phys.* **74**, 685 (1985).

<sup>15</sup> E. Eisenberg, S. Havlin, and G.H. Weiss, *Phys. Rev. Lett.* **72**, 2827 (1994).